Construction and Characterization of a Spectral Probe Mutant of Troponin C: Application to Analyses of Mutants with Increased Ca^{2+} Affinity†

Joyce R. Pearlstone,‡ Thor Borgford,‡,§ Murali Chandra,‡ Kim Oikawa,‡ Cyril M. Kay,‡ Osnat Herzberg,∥ John Moult,∥ André Herklotz,⊥ Fernando C. Reinach,⊥ and Lawrence B. Smillie*,‡

Medical Research Council Group in Protein Structure and Function, Department of Biochemistry, University of Alberta, Edmonton, Alberta, Canada T6G 2H7, Center for Advanced Research in Biotechnology, The Maryland Biotechnology Institute, University of Maryland, Rockville, Maryland 20850, and Departamento de Bioquimica, Instituto de Quimica, Universidade de Sao Paulo, CP 20.780, CEP 01498, Sao Paulo, Brazil

Received January 15, 1992; Revised Manuscript Received April 28, 1992

ABSTRACT: A spectral probe mutant (F29W) of chicken skeletal muscle troponin C (TnC) has been prepared in which Phe-29 has been substituted by Trp. Residue 29 is at the COOH-terminal end of the A helix immediately adjacent to the Ca^{2+} binding loop of site I (residues 30–41) of the regulatory N domain. Since this protein is naturally devoid of Tyr and Trp, spectral features can be assigned unambiguously to the single Trp. The fluorescent quantum yield at 336 nm is increased almost 3-fold in going from the Ca^{2+}-free state to the $4Ca^{2+}$ state with no change in the wavelength of maximum emission. Comparisons of the Ca^{2+} titration curves of the change in far-UV CD and fluorescence emission indicated that the latter was associated only with the binding of $2Ca^{2+}$ to the regulatory sites I and II. No change in fluorescence was detected by titration with Mg^{2+}. The Ca^{2+}-induced transitions of both the N and C domains were highly cooperative. Addition of Ca^{2+} also produced a red shift in the UV absorbance spectrum and a reduction in positive ellipticity as monitored by near-UV CD measurements. The fluorescent properties of F29W were applied to an investigation of five double mutants: F29W/V45T, F29W/M46Q, F29W/M48A, F29W/L49T, and F29W/M82Q. Ca^{2+} titration of their fluorescent emissions indicated in each case an increased Ca^{2+} affinity of their N domains. The magnitude of these changes and the decreased cooperativity observed between Ca^{2+} binding sites I and II for some of the mutants are discussed in terms of the environment of the mutated residues in the $2Ca^{2+}$ and modeled $4Ca^{2+}$ states. The observations are in general agreement with the proposed model (Herzberg, et al. (1986) *J. Biol. Chem. 261*, 2638–2644) for the Ca^{2+}-induced transition to the $4Ca^{2+}$ state.

Troponin C (TnC) is the Ca^{2+} binding component of the troponin complex which, together with troponin I and troponin T, is involved in the tropomyosin–actin thin filament regulation of skeletal and cardiac muscle contraction and relaxation [for reviews, see Leavis and Gergely (1984), Grand (1985), and Zot and Potter (1987c)]. The crystal structures of the turkey and chicken proteins have been elucidated by X-ray diffraction at atomic resolution (Herzberg & James, 1985a,b, 1988; Herzberg et al., 1986; Strynadka & James, 1989; Sundaralingam et al., 1985; Satyshur et al., 1988). The TnC molecule is visualized as an elongated dumbbell-shaped structure 75 Å in length with two globular domains connected by an exposed α-helix. Two metal binding sites, each arranged in a helix–loop–helix motif, are present in each of the N and C domains. Sites I and II, present in the N domain, are specific for Ca^{2+} and of relatively low affinity ($K_a \cong 10^5$–10^6 M^{-1}); sites III and IV of the C domain bind both Ca^{2+} and Mg^{2+} with higher affinity ($K_a \cong 10^7$ M^{-1} for Ca^{2+} and 10^3 M^{-1} for Mg^{2+}). In vivo, sites III and IV are believed to be invariably occupied by Ca^{2+}/Mg^{2+} and this domain is considered to play a structural role. Binding of Ca^{2+} to sites I and II of the N domain, however, is thought to be the regulatory event responsible for the triggering of muscle contraction. The Ca^{2+}-induced conformational transition is believed to be transmitted to the other members of the troponin complex (I and T), tropomyosin, and perhaps actin, thus facilitating thin filament and myosin interaction. Sequestration of Ca^{2+} by the sarcoplasmic reticulum reverses the process, leading to muscle relaxation. The structural transitions associated with Ca^{2+} binding to sites I and II of TnC and its release are thus of crucial importance to this system.

Since the TnC crystals were grown at ~pH 5, the regulatory sites I and II in the X-ray structures are unoccupied, whereas those in the C domain (III and IV) are filled with Ca^{2+}. On the basis of the assumption that the structure of the regulatory domain in the Ca^{2+}-bound state would be similar to that of the known C domain, Herzberg et al. (1986) proposed a model for the Ca^{2+}-induced structural transition of the regulatory domain. This conformational change would involve a reorganization of the secondary structural elements such that helices B and C move as a unit relative to the N, A, and D helices, the former and latter helices retaining their relative dispositions one to another. As a consequence, a number of nonpolar side chains of helices B, C, and D, totally or partially inaccessible to solvent in the $2Ca^{2+}$ state, become more exposed on the protein surface to form a "hydrophobic patch" in the $4Ca^{2+}$ state. This hydrophobic patch has been suggested as a possible site of interaction with other members of the troponin complex.

†This study was supported by grants from The Medical Research Council of Canada, FAPESP, FAPERJ, CNPq, FINEP, The Muscular Dystrophy Association U.S.A., and The Rockefeller Foundation. T.B. was supported by a postdoctoral fellowship from the Alberta Heritage Foundation for Medical Research and A.H. by an undergraduate fellowship from FAPESP.

‡University of Alberta.

§Present address: Department of Chemistry/Biochemistry, Simon Fraser University, Burnaby, BC, Canada V5A 1S6.

∥University of Maryland.

⊥Universidade de Sao Paulo.

0006-2960/92/0431-6545$03.00/0

In the present work we have prepared a mutated form of chicken skeletal muscle TnC (F29W) in which Trp serves as a spectral probe for monitoring the Ca^{2+}-induced structural transition of the regulatory domain. Since this protein is naturally devoid of Trp and Tyr, the mutation of Phe-29 to Trp allows the unambiguous assignment of spectral features to this residue. Upon Ca^{2+} binding a number of spectral features are altered, including an almost 3-fold increase in fluorescence quantum yield. This latter change has been shown to be highly cooperative and associated only with the N domain conformational transition. The spectral features of F29W have been successfully applied to an analysis of the Ca^{2+} binding affinities of five double mutants in which nonpolar hydrophobic patch amino acids at positions V45, M46, M48, L49, and M82 have been replaced by more polar residues. The prediction that such mutations would lead to a shift in the equilibrium from the $2Ca^{2+}$ to the $4Ca^{2+}$ states and thus to an increase in Ca^{2+} affinity has been validated. The observations are in general agreement with the proposed model (Herzberg et al., 1986) for the structural transition to the $4Ca^{2+}$ state.

Experimental Procedures

Construction of TnC Mutants and Protein Isolation. The construction of the expression vector and the preparation of TnC mutants by site-directed mutagenesis and their expression have been described (Reinach & Karlsson, 1988; Fujimori et al., 1990; Golosinska et al., 1991). All single mutants were entirely sequenced by the chain termination method (Sanger et al., 1977). The double mutants, each containing F29W, were produced by cloning, in turn, the unique Bst X1/Sal I fragments (starting at codon 41 and ending after the termination codon) of V45T, M46Q, M48A, L49T, and M82Q into the phosphatase-treated Bst X1/Sal I fragment of the F29W mutant of pLcII·FX·TnC. Each of the ligation mixes was transformed into cobalt-competent QY13. Correctness of the recombination was ascertained by plasmid sequencing using the sequenase enzyme of Tabor and Richardson (1987) in protocols described by Kraft et al. (1988) and the United States Biochemical Corp. (1987). Two primers were used to sequence the double mutants in the regions of F29W as well as codons 45–49 and 82.

Spectral Measurements. Stock buffer and protein solutions were prepared as previously described (Golosinska et al., 1991) with appropriate precautions for prevention of oxidation and contamination with Ca^{2+}. Following dialysis against 50 mM 3-(4-morpholino)propanesulfonic acid, 100 mM KCl, 1 mM [ethylenebis(oxyethylenenitrilo)]tetraacetic acid, 1 mM dithiothreitol, pH 7.1, stock protein solution (~2 mg/mL) was used either directly (UV difference absorbance spectroscopy and near-UV CD) or diluted with 0.22-μm-filtered outer dialysate buffer (far-UV CD and Trp fluorescence measurements). Final protein concentrations are given in the figure legends. CD spectra and titrations were described previously (Golosinska et al., 1991).

Difference absorbance spectra were determined at 20 °C on a Perkin-Elmer Lambda 5 recording spectrophotometer fitted with a thermostated cell compartment. Fluorescence measurements were conducted at 20 °C on a Perkin-Elmer MPF-44B fluorescence spectrophotometer operating in the ratio mode. Slit bandwidth was 5 nm for both excitation and emission. The A_{282} did not exceed 0.05, eliminating the need to make inner filter corrections. Measurements were with a 1-cm semimicrocell from Hellma, and detection was at right angles. Excitation λ was at 282 nm and emission λ_{max} at 336 nm. Calculation of free [Ca^{2+}] was as before (Golosinska et al., 1991) except that the log of the binding constant for TnC + 2Ca ⇌ TnC·2Ca was 13.4. A curve was fitted to the titration data by use of a nonlinear iterative least-squares procedure using an equation for one or two binding components as previously described (Golosinska et al., 1991).

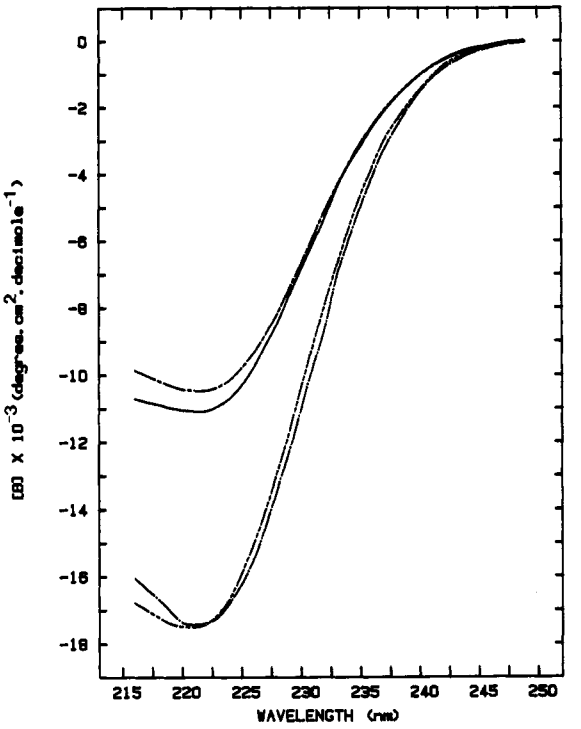

FIGURE 1: Far-UV CD spectra of recombinant TnC and F29W in the absence and presence of Ca^{2+}. Spectra were run in ±Ca^{2+} as described in Experimental Procedures: recombinant TnC (–Ca^{2+}, —; +Ca^{2+}, — --); F29W (–Ca^{2+}, —·; +Ca^{2+}, —·). Four experiments were carried out on both proteins (~33 μM) and the data shown are the averaged spectra in each case.

Results

Characterization of F29W. The far-UV CD spectra of recombinant TnC[1] and F29W in the absence and presence of Ca^{2+} are shown in Figure 1. The values of mean residue molar ellipticity at 221 nm for both proteins in the apo state (pCa of 8.8) are similar (~11 160 ± 960 and 10 530 ± 310, respectively), as is the increase in negative ellipticity upon the addition of Ca^{2+} to a pCa of 3.9 (final values of −17 560 ± 800 and −17 490 ± 590 for recombinant TnC and F29W, respectively). These values are similar to those reported by Johnson and Potter (1978) and McCubbin et al. (1982) for rabbit skeletal TnC.

Titration of the θ_{221nm} change of F29W as a function of pCa is shown in Figure 2. These data were best fitted by a biphasic curve in which ~65% of the total Ca^{2+}-induced ellipticity change was contributed by the binding of Ca^{2+} to the high-affinity domain and ~35% to the low-affinity domain. The four parameters describing this biphasic curve were as follows: for low-affinity sites, $-\log K_2 = 5.7$ and Hill coefficient $n = 2.0$; for high-affinity sites, $-\log K_1 = 6.7$ and $n = 1.9$ (see Table I). These values are similar to those we recently reported (Golosinska et al., 1991) for recombinant TnC and, taken together with the similar Ca^{2+}-induced ellipticity changes

[1] As previously documented (Golosinska et al., 1991), the deduced amino acid sequence of this recombinant TnC (after cleavage with factor Xa) differs from chicken muscle TnC at two positions. The blocking moiety (probably acetyl) at the NH_2 terminus of the naturally occurring muscle protein is replaced by Met; Thr-130 in muscle TnC is replaced by Ile.

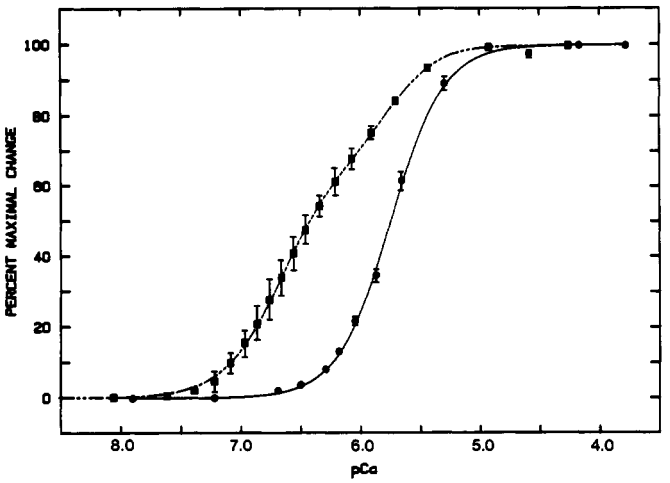

FIGURE 2: Ca^{2+} titrations of F29W monitored by far-UV CD and Trp fluorescence emission measurements. Far-UV CD (25° C, 29.7 μM protein); Trp fluorescence (20 °C, 3.3 μM protein). The averaged data points from three far-UV CD titrations are shown (■), with the range of values indicated by bars. The calculated fitted curve (— - -) for the data set was obtained by attributing 35% of the total ellipticity change to the low-affinity sites and 65% to the high-affinity sites. The Trp fluorescence titration curve (●, —) is the same as that of Figure 5 and represents the averaged values from two experiments.

Table I: Hill Coefficients and −log K Values for F29W and the F29W Double Mutants of TnC

	low-affinity site		high-affinity site	
mutant[a]	$-\log K_2$	n	$-\log K_1$	n
F29W	5.74 (±0.01)	1.99 (±0.07)	6.66 (±0.09)	1.88 (±0.02)
F29W	5.73 (±0.01)	1.97 (±0.08)		
F29W/V45T	5.94 (±0.01)	1.84 (±0.10)		
F29W/M46Q	6.01 (±0.00)	1.77 (±0.02)		
F29W/M48A	5.84 (±0.05)	1.41 (±0.14)		
F29W/L49T	6.06 (±0.11)	1.48 (±0.14)		
F29W/M82Q	6.16 (±0.00)	1.43 (±0.02)		

[a] Data were obtained from Ca^{2+} titrations of far-UV CD (the first row of data for F29W) and fluorescence emission. The data sets from each of three titrations for far-UV CD results and two or three titrations for fluorescence results were analyzed separately by means of a nonlinear iterative least-squares procedure (Golosinska et al., 1991), using the following equation for two binding components: $f = f_1\,[[Ca]^{n_1}/(K_1^{n_1} + [Ca]^{n_1})] + f_2[[Ca]^{n_2}/(K_2^{n_2} + [Ca]^{n_2})]$, where f is the percentage change in spectral feature, f_1 and f_2 are the percentages of total change attributed to the high- and low-affinity sites, respectively, n_1 and n_2 are the Hill coefficients, and K_1 and K_2 are the apparent dissociation constants. For the far-UV CD titrations, f_1 and f_2 were taken as 65% and 35%. For the fluorescence titrations these were taken as 0% and 100%, respectively. Deduced values of $-\log K$ and n from these analyses were averaged and presented above with standard deviations in brackets.

described above for both proteins, indicate that the substitution of Phe-29 by Trp has had little effect on the overall secondary structural features of the protein or on the Ca^{2+} affinity of the four Ca^{2+} binding sites.

The Trp fluorescence spectra of F29W in the absence and presence of Ca^{2+} are shown in Figure 3. Excitation was at 282 nm and emission maxima of both the $\pm Ca^{2+}$ states was at 336 nm. There was an almost 3-fold increase in relative fluorescence intensity in going from a pCa of 7.9 to 3.8. By use of a quantum yield of 0.13 (Eisinger, 1969) for free Trp as a standard in the same buffer, the quantum yield of F29W increased from 0.12 (apo) to 0.33 ($+Ca^{2+}$).

When the fluorescence intensity was monitored as a function of pCa (see Figures 2 and 5), a monophasic curve was obtained with a $-\log K_2$ of 5.7 and Hill coefficient $n = 2.0$ (see Table I). These parameters are in excellent agreement with the values obtained for the low-affinity sites from the far-UV CD titration data (see Figure 2 and Table I). This good agreement indicates that the Trp fluorescence is serving as a useful probe

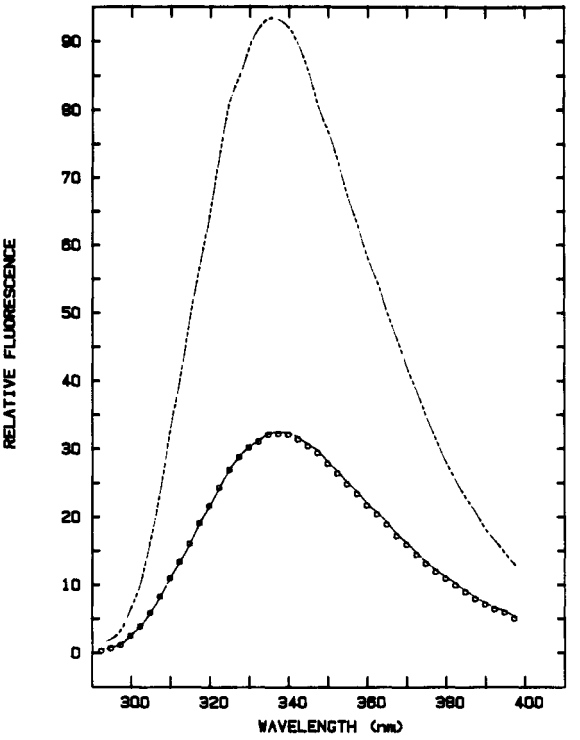

FIGURE 3: Emission fluorescence spectra of F29W in $-Ca^{2+}$, $+Mg^{2+}$ and Ca^{2+}/Mg^{2+}. Excitation was at 282 nm. The data were normalized using a Trp quantum yield of 0.13 as standard (Eisinger, 1969). Buffer conditions were the same as in Experimental Procedures. The three spectra were with no Ca^{2+} (—), Mg^{2+} added to 46 mM (○) and Ca^{2+} added to 2 mM (— - -). Protein concentration was 5.1 μM.

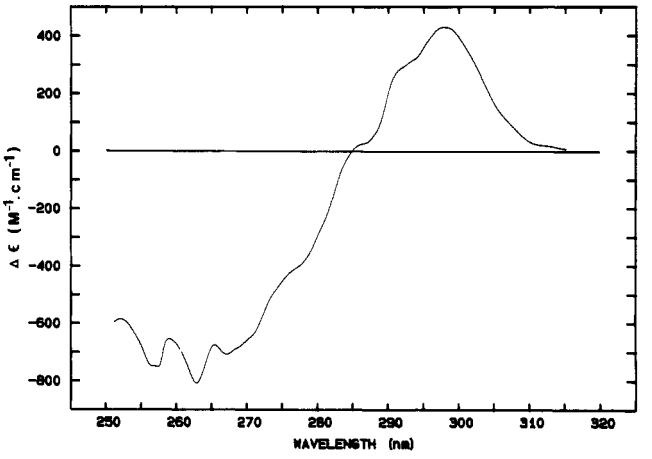

FIGURE 4: Ultraviolet difference absorption spectrum of F29W upon addition of Ca^{2+}. Buffer conditions were as in Experimental Procedures; temperature 21 °C; protein concentration 90.7 μM. Data were corrected for dilution and are expressed as the change in molar extinction coefficient, Δε.

for monitoring the Ca^{2+}-induced structural transition of the regulatory domain and that its environment is not significantly affected by Ca^{2+}-induced structural changes at sites III and IV. This latter conclusion is further substantiated by titration of F29W with Mg^{2+}. No change in the fluorescence properties of F29W was detected up to a concentration of 46 mM Mg^{2+} (see Figure 3).

That the local environment of Trp-29 is altered by the Ca^{2+}-induced structural transition is also shown by UV difference absorbance spectroscopy (Figure 4). When a saturating level of Ca^{2+} (2 mM) was added to the sample cuvette and an equal volume of water added to the reference cell to maintain equal concentration of protein and EGTA (1 mM) in both cells, a positive difference was observed in the UV

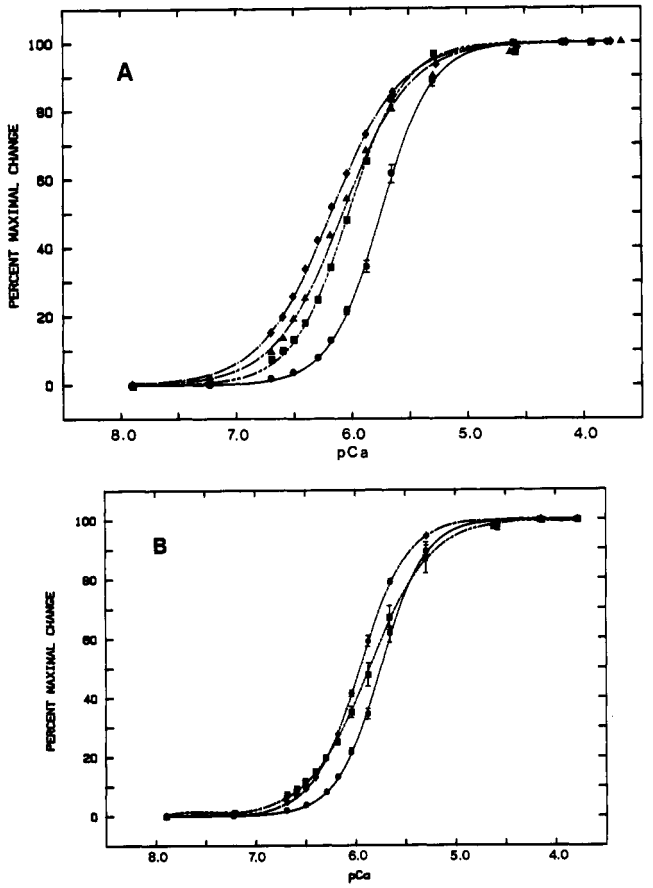

FIGURE 5: Calcium titration curves of Trp fluorescence intensities of F29W and the F29W hydrophobic patch mutants. Buffer conditions were as in Experimental Procedures; temperature 20 °C; protein concentrations were in the range of 2.8–3.6 μM. Panel A: F29W (●, —); F29W/M46Q (■, —--); F29W/L49T (▲, —-); F29W/M82Q (◆, —·). Panel B: F29W (●, —); F29W/V45T (◆, —-); F29W/M48A (■, —--). For each mutant, the averaged values for two or three titrations are shown by symbols and the final calculated fitted curves by lines. The ranges of values for F29W in panel A and for all three mutants in panel B are shown by vertical bars. In panel A, these have been omitted for the three double mutants for the sake of clarity but were in the same range as F29W.

region corresponding to Trp absorbance bands. Such a red shift in Trp absorbance in normally attributed to a change to a more nonpolar environment of the indole ring (Donovan, 1969). The contribution to the difference spectrum of Phe residues (five in the C domain and five in the N domain) is seen at lower wavelengths in the region of 250–275 nm.

A local Ca^{2+}-induced change in the environment of Trp-29 is also indicated by measurements of the near-UV CD spectrum of F29W (see Figure 6). The positive ellipticity for the apo state over the wavelengths 270–295 nm is seen to be reduced to close to zero or to negative values when Ca^{2+} is added to saturating levels.

Characterization of the Double Hydrophobic Patch Mutants. Ca^{2+} titration of the fluorescence change for each of these double mutants as well as for the F29W control is shown in Figure 5. In each case an increase in Ca^{2+} affinity from a $-\log K_2$ of 5.7 for F29W to values varying from 5.8 to 6.2 is demonstrated (Table I). In addition, the cooperativity as estimated by the value of the Hill coefficient n is seen to be significantly decreased for several of these mutants.

The near-UV CD spectra for F29W and each of the double mutants in the absence and presence of Ca^{2+} are shown in Figure 6A and B, respectively. In the absence of Ca^{2+} all six proteins show a rather broad featureless positive ellipticity peak in the region of 270–300 nm. In the presence of Ca^{2+} the six

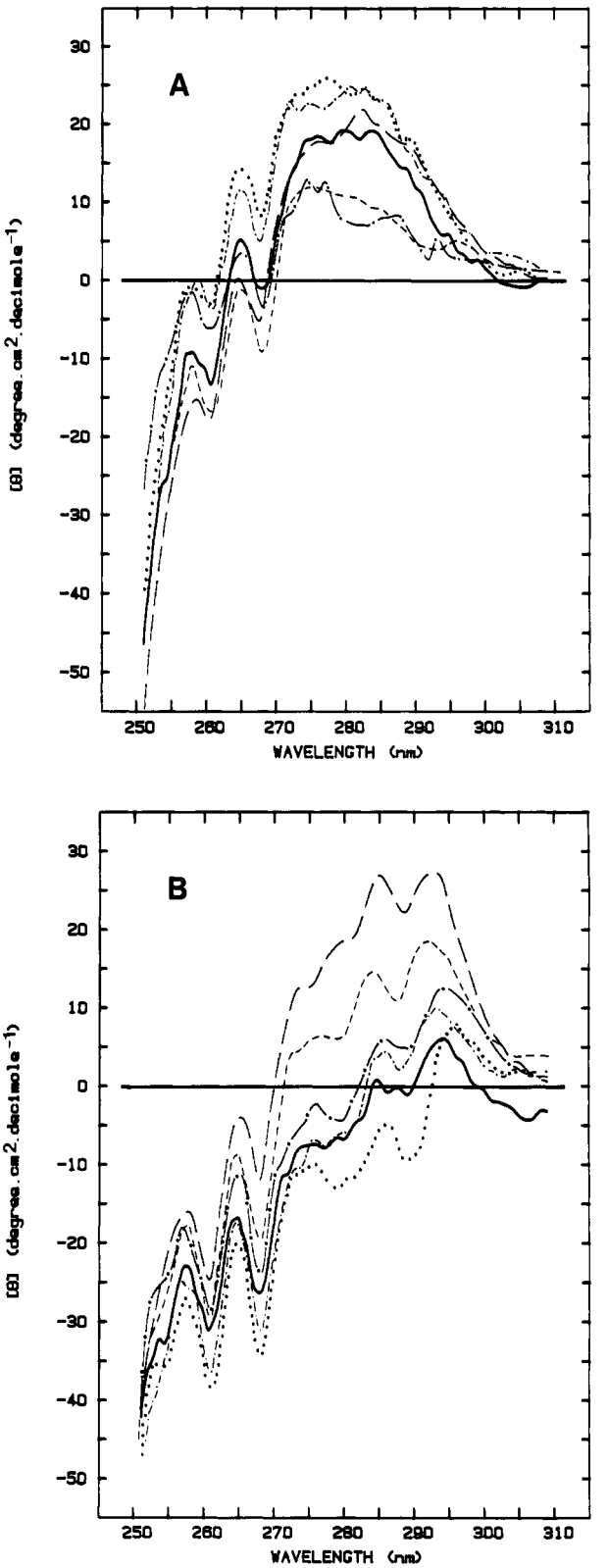

FIGURE 6: Near-UV CD spectra of F29W and hydrophobic patch double mutants in the absence of Ca^{2+} (panel A) and the presence of Ca^{2+} (panel B). Protein concentrations were in the range of 55–84 μM. F29W (—); F29W/V45T (--); F29W/M46Q (—·—); F29W/M48A (---); F29W/L49T (—··—); F29W/M82Q (···).

spectra are characterized by ellipticity peaks at 295 and 286 nm. However, the magnitude of the molar ellipticities of these features varies significantly for the six proteins. These data suggest that while the six mutants are not identical in terms of the environment of the Trp side chain, the differences are probably of a rather subtle nature. They also indicate that

the environment change of the indole ring in the Ca^{2+}-induced transitions is rather similar in each case.

Discussion

In the present work we have shown that a mutant of TnC in which Phe-29 is mutated to Trp can serve as a sensitive fluorescent probe for monitoring the Ca^{2+}-induced structural transition of its regulatory N domain. The spectral properties of the probe appear to be unaffected by Ca^{2+} or Mg^{2+} binding to the C domain (sites III and IV) nor is the overall secondary structure of the protein apparently altered by the substitution. Neither the Ca^{2+} affinity nor the cooperativity between sites I and II is significantly affected by the mutation. We have also demonstrated the usefulness of this probe in monitoring the effects of five secondary mutants, in which nonpolar residues are replaced by more polar amino acids, in a region of the protein postulated to become more accessible to solvent as a result of the Ca^{2+}-induced structural transition.

Spectral probe techniques for monitoring of structural transitions in TnC and other proteins have been widely and usefully applied. In some studies this has involved the introduction of an extrinsic spectral feature by chemical and, hopefully, specific derivatization of a residue side chain, usually that of cysteine or methionine. Such probes however are generally of a complex aromatic nonpolar nature and have the potential for strong interaction with hydrophobic regions of the protein. By virtue of this property, and, in the case of methionine, the introduction of a positively charged sulfonium ion as a result of the derivatization reaction, significant protein structural alterations can be expected in some cases.

Alternatively the spectral properties of naturally occurring tyrosine and/or tryptophan residues can serve as useful monitors of protein structural transitions. This approach is the least invasive, of course, but interpretation can be difficult in those cases in which a number of such residues are present. Both approaches are limited to those regions of the molecule containing residues which can be successfully derivatized or in which the naturally occurring tyrosine and tryptophan are located.

Properties of F29W TnC. In the present study we have used site-directed mutation to substitute Phe-29 by a single tryptophan residue in recombinant chicken TnC. Since this protein is naturally devoid of both tryptophan and tyrosine, a number of spectral properties can be unambiguously assigned to this residue. The most useful of these properties has been an almost 3-fold increase in quantum yield of fluorescence associated with the Ca^{2+}-induced structural transition of the N domain. In the naturally occurring protein, Phe-29 occupies a position at the COOH-terminal end of the A helix, immediately adjacent to the Ca^{2+}-binding loop (residues 30–41) of binding site I (see Figure 7). In the crystal structure of the $2Ca^{2+}$ state of the protein, its side chain is only partially accessible to solvent and has extensive interactions with a number of neighboring residues in its immediate environment. These include the side chains of Met-28, Ile-37, Glu-41, Thr-44, Val-45, and Met-48. Following the Ca^{2+}-induced structural transition, the hypothetical model predicts a new set of interactions involving Ala-25, Ile-37, Val-45, and Phe-78. In both the apo and Ca^{2+}-bound states, all side-chain carbon atoms of Phe-29 would be involved in van der Waals interactions. Only a very modest increase in solvent accessibility of Phe-29 (from 46.2 to 55.7 Å^2) is predicted for the Ca^{2+}-induced transition.

In light of these extensive interactions with neighboring residues, in both conformational states, it would be unrealistic not to anticipate some local disruption of the immediate environment when Phe is replaced by Trp. Indeed, inspection of the crystal structure of the apo form shows that some displacement of side chains is required to sterically accommodate a Trp side chain at this position. This would be true for both the determined and modeled structures. However, present evidence suggests that the global properties of the molecule are not markedly affected by the substitution. Thus the similar far-UV CD spectra of the wild-type and F29W proteins indicate that their secondary structural features are very similar in both the apo and Ca^{2+}-bound states. Further, their affinity for Ca^{2+}, as well as the cooperativity of the Ca^{2+}-induced structural transitions as assessed by far-UV CD measurements, is the same within experimental error. The minimal effects of the Trp for Phe substitution have also been substantiated by the absence of a significant difference in tension measurements when F29W replaces either recombinant or chicken muscle TnC in rabbit skinned fibers.[2] We have also recently demonstrated that the reconstitution of F29W into a rabbit troponin–tropomyosin–actomyosin S1 ATPase, as a replacement for muscle TnC, has little effect on the Ca^{2+} sensitivity of that system.[3]

Cooperativity. One of the more important features of the present observations is the high level of cooperativity observed in the Ca^{2+} titration curves attributable to both the low-affinity sites I and II and the high-affinity sites III and IV (see Table I). As shown by Grabarek and Gergely (1983), Hill coefficients of $n \geq 1.4$ can only be ascribed to positive cooperativity between the two sites and not to complications arising from differential contributions to the fluorescence change by metal binding to the two sites. Evidence in the literature bearing on the question of cooperativity between these paired sites has been contradictory. Reports have included evidence for four independent and noninteracting sites (Potter & Gergely, 1975; Ogawa, 1985) and for cooperativity between sites III and IV (Leavis et al., 1978; Jahnke & Heilmeyer, 1980; Teleman et al., 1983; Grabarek et al., 1983, 1986, 1990; Iida, 1988). Either no evidence was obtained for cooperativity between sites I and II or the question could not be addressed on the basis of the available experimental evidence. These reports are surprising in light of the now documented extensive interaction of the pairs of sites in both the N and C domains of the crystal structures (Strynadka & James, 1989) as well as the close structural coupling of sites I and II in the melting profiles of the N domain (Tsalkova & Privalov, 1985). Only recently (Putkey et al., 1989; Sheng et al. 1990) have site-specific mutations in sites I and II provided evidence for cooperativity between these sites. Previous studies may have been compromised, we suspect, by one or more of several factors. In the case of direct binding measurements by equilibrium dialysis, reproducibility of data points is a major problem. Because of the errors involved, the quality of the experimental binding curves may be inadequate to reliably distinguish between interacting and noninteracting sites. The problem may be further compounded by the effects of oxidation of methionine and/or cysteine residues during the long periods of dialysis normally necessary to attain the equilibrium state. Even if reducing conditions are initially present, often not the case, these may be short-lived by virtue of the relatively short half-life of the usual reducing agents in neutral or alkaline solution exposed to the atmosphere. In the present report, and in our continuing studies, we have found that reproducible titrations of the spectral properties are dependent on maintaining a reducing environment, both during the protein

[2] Personal communication: M. Sorenson.

[3] Unpublished data: J. A. Ferro and L. B. Smillie.

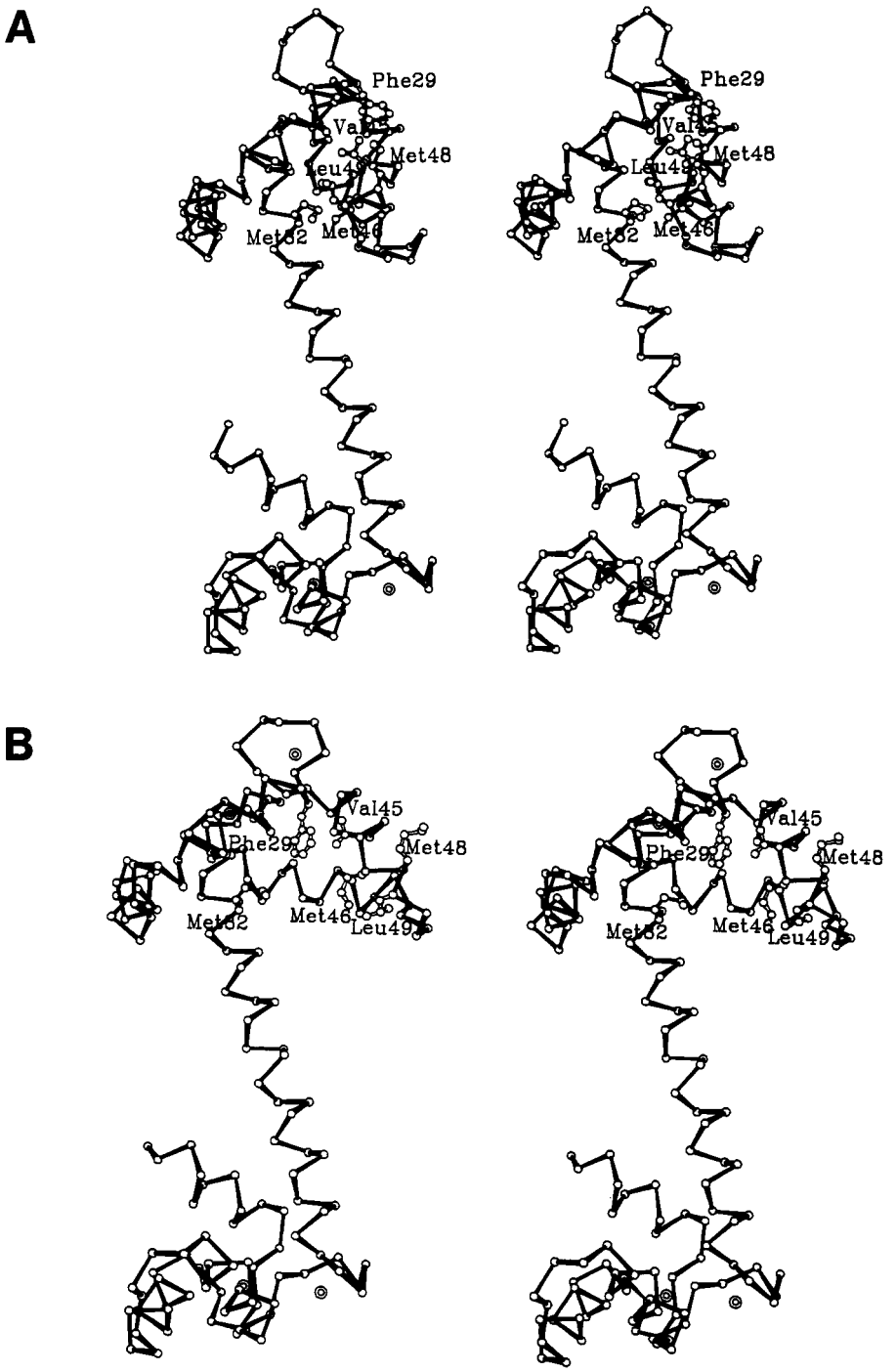

FIGURE 7: Stereographic representations of the α-carbons of the crystal structure of TnC in the $2Ca^{2+}$ state (A) and the proposed $4Ca^{2+}$ state (B). The concentric circles are Ca^{2+} atoms. The side chains of residues F29, V45, M46, M48, L49, and M82 are shown. The model for the $4Ca^{2+}$ state is based on the assumption that, upon binding of an additional two Ca^{2+} ions, the N domain of the molecule undergoes a conformational transition to become closely similar in structure to the C domain which always binds Ca^{2+} or Mg^{2+} under physiological conditions (Herzberg et al., 1986).

preparation and during the analyses themselves. The importance of this precaution is consistent with early reports (Walsh & Stevens, 1977, 1978) that the functional and Ca^{2+} binding properties of calmodulin are dramatically altered by methionine oxidation and the now known structural role of methionines in the polypeptide chain packing of TnC.

The lack of cooperativity between sites I and II observed in previous studies may be related in another way to this question of integrity of the methionine side chains. A derivative of TnC with dansylaziridine, in which Met-25 of rabbit TnC (Met-28 in chicken TnC) is derivatized to form the sulfonium salt, has been used effectively and extensively as a fluorescent probe for monitoring the Ca^{2+}-induced structural transitions of its regulatory domain (Johnson et al., 1978, 1979; Potter et al., 1981; Grabarek et al., 1983, 1990; Griffiths et al., 1984; Zot et al., 1986; Zot & Potter, 1987a,b, 1989; Güth & Potter, 1987; Ellis et al., 1988). In contrast to the present results, these studies observed no cooperativity in the Ca^{2+}-induced transition [see, for example, Grabarek et al. (1990)]. Although this methionine is largely exposed to solvent both in the crystal and in the modeled $4Ca^{2+}$ state, the introduction of a large aromatic nonpolar moiety as well as a positive charge on the sulfur of the side chain may well be responsible for this apparent loss of site interactions. The present results with the F29W double mutants indicate that this cooperativity in some cases is decreased significantly by even relatively conservative

single amino acid substitutions at certain locations in the protein structure. These observations suggest that even minor structural modifications of the regulatory domain can lead to changes in site I and II interactions and cooperativity of Ca^{2+} binding to the sites.

Design of Hydrophobic Patch Mutants. In the Ca^{2+}-induced structural transition proposed by Herzberg et al. (1986), a number of nonpolar side chains undergo changes in their interactions and environment such that they become more exposed on the surface of the protein to produce a nonpolar or hydrophobic patch. The unfavorable energetics of this exposure of nonpolar residues to solvent is presumed to be compensated by the binding of Ca^{2+}. The Ca^{2+} affinity of the regulatory domain sites I and II is thus predicted to be coupled to the change in energy associated with this increased exposure to solvent of these nonpolar residues. A reduction in the energy required to drive this structural transition would be expected to appear as an increase in Ca^{2+} affinity. Such a reduction in energy and increased affinity should, in theory, be achievable by a reduction in the nonpolar characteristics of the hydrophobic patch. The five double mutants described in the present paper were chosen to test this prediction. Their location in the three-dimensional structure is shown in Figure 7.

The exact choice of mutants involved a number of considerations. Thus, in addition to the question of increased surface hydrophilicity/hydrophobicity of a particular mutant, it was necessary to assess its potential for stabilization/destabilization of the $2Ca^{2+}$ and $4Ca^{2+}$ states. For example, mutation to a more bulky side chain of a nonpolar residue fully buried in the $2Ca^{2+}$ state but exposed in the $4Ca^{2+}$ state would be expected to lead to local disruption of the former state and therefore to an increase in Ca^{2+} affinity. To avoid this "wedge" effect, mutants were chosen such that side-chain volume was kept similar or, in some cases, reduced. Other considerations were the effects on stability of the introduction of a polar side chain into a buried nonpolar environment and of the reduction of surface hydrophobicity of a shorter nonpolar side chain on the stabilities of the two states. Such effects for each mutant are considered below.

Mutant V45T. This is the most conservative mutation. In the crystal structure of the $2Ca^{2+}$ state, this valine is completely inaccessible to solvent. After transition to the $4Ca^{2+}$ state, exposure of the two side-chain methyl groups (Cγ1 and Cγ2) is predicted to lead to an increase of surface accessibility to solvent (Herzberg et al., 1986) (Figure 7). Minimal change in side-chain volume occurs when Thr replaces Val. A model of the mutant shows that, in the $2Ca^{2+}$ state, the polarity of the Thr side chain may be satisfied by hydrogen bonding with the main-chain oxygen of residues 41 and 42 and with the main-chain nitrogen of residue 46. Replacement of Val-45 by Thr is therefore not expected to seriously destabilize the $2Ca^{2+}$ state. In the $4Ca^{2+}$ state the hydroxyl (Oγ) and methyl group (Cγ) of the Thr side chain would be accessible to solvent. Thus the observed increase in $-\log K_2$ value (Table I) can probably be largely ascribed to the reduced hydrophobic surface of the $4Ca^{2+}$ state of the latter mutant. No significant reduction in Hill coefficient (n) and thus in the cooperativity of the transition was seen in this case.

Mutants M46Q and M82Q. In the $2Ca^{2+}$ state both of these methionines are fully buried and inaccessible to solvent. Following transition to the $4Ca^{2+}$ state, the model predicts that the two side chains become exposed to solvent. The replacement of M by Q leads to a minimal change in side-chain volume but for both mutants introduces a polar moiety into a nonpolar environment of the $2Ca^{2+}$ state. Inspection of the modeled mutants shows that in neither case are there potential hydrogen bond acceptors/donors available in the immediate environment for interaction with the introduced polar moiety. Thus, an increase in Ca^{2+} affinity due to decreased hydrophobicity in the $4Ca^{2+}$ would be expected to be reinforced by some destabilization of the $2Ca^{2+}$ state. The observed increases in $-\log K_2$ values from 5.7 for F29W to 6.0 for F29W/M46Q and 6.2 for F29W/M82Q (see Table I) are in general agreement with this interpretation. For M82Q, a significant reduction in the cooperativity of the transition is observed (Hill coefficient reduced to 1.4 from 1.9), probably reflecting the different structural positions of the two methionines in the $2Ca^{2+}$ and $4Ca^{2+}$ protein structures. Such interpretations must be tempered with the realization that the $4Ca^{2+}$ protein structure represents a model and not an experimental result. While all evidence to date suggests that its general features are valid, it is unlikely to be correct in all details.

Mutant L49T. In the crystal structure of the $2Ca^{2+}$ state, this leucine side chain is partially exposed (solvent accessibility value of 28 Å^2). In the model of the $4Ca^{2+}$ state, the side-chain exposure increases substantially (98.2 Å^2) (Herzberg et al., 1986). As well as introducing a more hydrophilic side chain, the L49T mutation reduces side-chain volume. Inspection of the modeled mutant in the $2Ca^{2+}$ state shows that the Oγ of Thr could hydrogen bond to the main-chain oxygen of residue 45 leaving the Cγ of Thr exposed to solvent. Alternatively, the O could assume an exposed position. In the modeled $4Ca^{2+}$ state, several alternative interactions of the Oγ and Cγ could be assumed in which the oxygen is either exposed or interacts with the main-chain oxygen of residue 46. This, therefore, is a more complex situation than for the other mutants. Nevertheless, the total effect of the mutation is that the hydrophobic atom exposure is reduced in the $4Ca^{2+}$ state. The fluorescence data demonstrate that a significant increase in Ca^{2+} affinity occurs (see Table I), roughly equivalent to that of the two MQ mutants, and that cooperativity is reduced.

Mutant M48A. In both the $2Ca^{2+}$ and modeled $4Ca^{2+}$ states, this methionine residue is largely exposed to solvent (96 and 138 Å^2, respectively). Since the replacement of the side chain of Met by Ala largely removes the nonpolar characteristics of this residue in both the $2Ca^{2+}$ and $4Ca^{2+}$ states, we would expect minimal change in hydrophobic surface area resulting from the Ca^{2+}-induced structural transition. This expectation is consistent with the observation that this mutant, among those tested, shows the smallest increase in $-\log K_2$ and therefore Ca^{2+} affinity. Examination of the data of Table I shows that the $-\log K_2$ value (5.8) for F29W/M48A is only marginally increased from that of F29W ($-\log K_2 = 5.7$). At present we have no explanation for the reduced cooperativity observed with this mutant.

In summary, the fluorescence titration data of all five F29W double mutants are consistent with predictions based on the model of the calcium-induced structural transition and on the local structural environment of the individual amino acid residues in the $2Ca^{2+}$ and $4Ca^{2+}$ states. This is particularly true of the three mutants M46Q, M82Q, and V45T, in which there is minimal side-chain volume change and in which the naturally occurring side chains are completely inaccessible to solvent in the $2Ca^{2+}$ state. In the case of the two M to Q mutants, some destabilization of the $2Ca^{2+}$ state would be expected since the polar moiety of Q is being introduced into a nonpolar environment. An increased affinity for Ca^{2+} would result from both this destabilization and a decreased nonpolar surface exposure in the $4Ca^{2+}$ state. In the case of the Val to Thr mutation, the polarity of the Oγ atom can be at least

partially satisfied by H bonding to main-chain oxygen or nitrogen atoms. Therefore no destabilization should be expected for the $2Ca^{2+}$ state. Consistent with this argument, the fluorescence titration data clearly show that the two M to Q mutants have a larger effect on calcium affinity than the V45T mutation. Comparison of the effects of the M48A mutation with those of the above three mutants is also understandable in these terms. This Met is largely exposed to solvent in both the $2Ca^{2+}$ and $4Ca^{2+}$ states. Removal of the bulk of the side chain by mutation to Ala would thus result in a situation in which there would be little increase of nonpolar surface in going to the fully Ca^{2+} loaded state. This mutant showed the smallest effect on Ca^{2+} affinity (Table I) but the largest reduction in Hill coefficient.

In conclusion, the mutation of Phe-29 to Trp in chicken skeletal muscle TnC appears not to have altered the overall structural features of the protein nor to have altered significantly its Ca^{2+} binding properties. The Ca^{2+}-induced structural transition of the protein's N domain is accompanied by changes in several spectral features including an almost 3-fold increase in fluorescence emission at 336 nm. Ca^{2+} titrations of this change in fluorescence as well as in the circular dichroism properties of the protein have shown a high level of cooperativity between Ca^{2+} binding sites I and II and between sites III and IV. Both the Ca^{2+} titration data and the absence of effects of Mg^{2+} concentration show that the fluorescence changes are associated specifically with structural transitions in the N domain and appear not to be affected by Ca^{2+}/Mg^{2+}-induced changes in the C domain.

The spectral features of the F29W mutant have been usefully applied in monitoring the Ca^{2+} binding affinities of five double mutants, each containing F29W and in which nonpolar hydrophobic patch residues have been mutated to amino acids with more polar side chains. The prediction that these would shift the equilibrium from the $2Ca^{2+}$ and $4Ca^{2+}$ state and thus lead to a higher Ca^{2+} affinity of sites I and II has been validated. The relative magnitudes of the changes in the Ca^{2+} affinity for each double mutant and the decreases in observed cooperativity observed with some of them have been discussed in terms of the environment of each mutated residue in the $2Ca^{2+}$ and modeled $4Ca^{2+}$ states. The results are the first to demonstrate increases in Ca^{2+} binding by mutation of appropriate residues in the TnC molecule. Previous mutations (Fujimori et al., 1990; Grabarek et al., 1990) were designed to stabilize the $2Ca^{2+}$ state by either the formation of a disulfide bond or the creation of an additional salt linkage in the known tertiary structure of the protein. However the observed decreases in Ca^{2+} affinity, while consistent with the hypothetical model for the transition, could also have arisen by secondary structural perturbations not necessarily directly related to a shift in equilibrium in the direction of the $2Ca^{2+}$ state. The increase in Ca^{2+} affinity observed with the present mutants is less likely to have arisen from such nonspecific effects and is certainly consistent with the general features of the postulated model.

Acknowledgments

We are indebted to Drs. N. C. J. Strynadka and M. N. G. James for helpful discussions.

Registry No. Ca^{2+}, 7440-70-2; Met, 63-68-3; Gln, 56-85-9; Val, 72-18-4; Thr, 72-19-5; Ala, 56-41-7; Leu, 61-90-5.

References

Donovan, J. W. (1969) in *Physical Principles and Techniques of Protein Chemistry* (Leach, S. J., Ed.), pp 101–170, Academic Press, New York.

Eisinger, J. (1969) *Photochem. Photobiol. 9*, 247–259.

Ellis, P. D., Marchetti, P. S., Strang, P., & Potter, J. D. (1988) *J. Biol. Chem. 263*, 10284–10288.

Fujimori, K., Sorenson, M., Herzberg, O., Moult, J., & Reinach, F. (1990) *Nature 345*, 182–184.

Golosinska, K., Pearlstone, J. R., Borgford, T., Oikawa, K., Kay, C. M., Carpenter, M. R., & Smillie, L. B. (1991) *J. Biol. Chem. 266*, 15797–15809.

Grabarek, Z., & Gergely, J. (1983) *J. Biol. Chem. 258*, 14103–14105.

Grabarek, Z., Grabarek, J., Leavis, P. C., & Gergely, J. (1983) *J. Biol. Chem. 258*, 14098–14102.

Grabarek, Z., Leavis, P. C., & Gergely, J. (1986) *J. Biol. Chem. 261*, 608–613.

Grabarek, Z., Tan, R.-Y., Wang, J., Tao, T., & Gergely, J. (1990) *Nature 345*, 132–135.

Grand, R. J. A. (1985) *Top. Mol. Struct. Biol. 7*, 65–122.

Griffiths, P. J., Potter, J. D., Coles, B., Strang, P., & Ashley, C. C. (1984) *FEBS Lett. 176*, 144–150.

Güth, K., & Potter, J. D. (1987) *J. Biol. Chem. 262*, 13627–13635.

Herzberg, O., & James, M. N. G. (1985a) *Nature 313*, 653–659.

Herzberg, O., & James, M. N. G. (1985b) *Biochemistry 24*, 5298–5302.

Herzberg, O., & James, M. N. G. (1988) *J. Mol. Biol. 203*, 761–768.

Herzberg, O., Moult, J., & James, M. N. G. (1986) *J. Biol. Chem. 261*, 2638–2644.

Iida, S. (1988) *J. Biochem. (Tokyo) 103*, 482–486.

Jahnke, U., & Heilmeyer, L. M. G. (1980) *Eur. J. Biochem. 111*, 325–332.

Johnson, J. D., & Potter, J. D. (1978) *J. Biol. Chem. 253*, 3775–3777.

Johnson, J. D., Collins, J. H., & Potter, J. D. (1978) *J. Biol. Chem. 253*, 6451–6458.

Johnson, J. D., Charlton, S. C., & Potter, J. D. (1979) *J. Biol. Chem. 254*, 3497–3502.

Kraft, R., Tardiff, J., Krauter, K. S., & Leinwand, L. A. (1988) *Biotechniques 6*, 544–547.

Leavis, P. C., & Gergely, J. (1984) *CRC Crit. Rev. Biochem. 16*, 235–305.

Leavis, P. C., Rosenfeld, S. S., Gergely, J., Grabarek, Z., & Drabikowski, W. (1978) *J. Biol. Chem. 253*, 5452–5457.

McCubbin, W. D., Oikawa, K., Sykes, B. D., & Kay, C. M. (1982) *Biochemistry 21*, 5948–5956.

Ogawa, Y. (1985) *J. Biochem. (Tokyo) 97*, 1011–1023.

Potter, J. D., & Gergely, J. (1975) *J. Biol. Chem. 250*, 4628–4636.

Potter, J. D., Charlton, S. C., & Johnson, J. D. (1981) *Fed. Proc. 40*, 2653–2656.

Putkey, J. A., Sweeney, H. L., & Campbell, S. T. (1989) *J. Biol. Chem. 264*, 12370–12378.

Reinach, F. C., & Karlsson, R. (1988) *J. Biol. Chem. 263*, 2371–2376.

Sanger, F., Nicklen, S., & Coulson, R. (1977) *Proc. Natl. Acad. Sci. U.S.A. 74*, 5463–5467.

Satyshur, K. A., Rao, S. T., Pyzalska, D., Drendel, W., Greaser, M., & Sundaralingam, M. (1988) *J. Biol. Chem. 263*, 1628–1647.

Sheng, Z., Strauss, W. L., Francois, J.-M., & Potter, J. D. (1990) *J. Biol. Chem. 265*, 21554–21560.

Strynadka, N. C. J., & James, M. N. G. (1989) *Annu. Rev. Biochem. 58*, 951–998.
Sundaralingam, M., Bergstrom, B., Strasburg, G., Rao, S. T., Roychowdhury, P., Greaser, M., & Wang, B. C. (1985) *Science 227*, 945–948.
Tabor, S., & Richardson, C. C. (1987) *Proc. Natl. Acad. Sci. U.S.A. 84*, 4767–4771.
Teleman, O., Drakenberg, T., Forsén, S., & Thulin, E. (1983) *Eur. J. Biochem. 134*, 453–457.
Tsalkova, T. N., & Privalov, P. L. (1985) *J. Mol. Biol. 181*, 533–544.
United States Biochemical Corp. (1987) *Step-by-Step Protocols for DNA Sequencing with Sequenase*, 3rd ed., Cleveland, OH 44122.
Walsh, M., & Stevens, F. C. (1977) *Biochemistry 16*, 2742–2747.
Walsh, M., & Stevens, F. C. (1978) *Biochemistry 17*, 3924–3930.
Zot, A. S., & Potter, J. D. (1987a), *J. Biol. Chem. 262*, 1966–1969.
Zot, H. G., & Potter, J. D. (1987b) *J. Muscle Res. Cell Motil. 8*, 428–436.
Zot, A. S., & Potter, J. D., (1987c) *Annu. Rev. Biophys. Biochem. 16*, 535–559.
Zot, H. G., & Potter, J. D. (1989) *Biochemistry 28*, 6751–6756.
Zot, H. G., Güth, K., & Potter, J. D. (1986) *J. Biol. Chem. 261*, 15583–15890.

Inhibitors of Protein Phosphatase Type 1 and 2A Attenuate Phosphatidylinositol Metabolism and Ca^{2+}-Transients in Human Platelets. Role of a cdc2-Related Protein Kinase†

Kenneth M. Lerea
Department of Cell Biology and Anatomy, Basic Sciences Building, New York Medical College, Valhalla, New York 10595
Received February 12, 1992; Revised Manuscript Received April 17, 1992

ABSTRACT: The addition of either okadaic acid or calyculin A desensitizes human platelets to thrombin. One objective of this study was to determine which step(s) leading to secretion reactions may be affected by these protein phosphatase inhibitors. In a dose-dependent manner, okadaic acid or calyculin A inhibits phosphatidylinositol metabolism and Ca^{2+}-transients. In all cases, calyculin A was approximately 10-fold more potent than okadaic acid, and it had maximal effects at a concentration of 1 μM. Although thrombin-induced rises in $[Ca^{2+}]_i$ were diminished, an increase in the phosphorylation state of myosin light chains (MLC) was still observed. Changes in this phosphorylation were diminished, however, following the addition of thrombin to calyculin A-treated platelets that were loaded with dimethyl-BAPTA. These data demonstrate that calyculin A and okadaic acid lower agonist-induced Ca^{2+}-transients, which in turn prevents responses such as secretion reactions. Calyculin A/okadaic acid-induced phosphorylation events were not diminished in BAPTA-loaded platelets, suggesting that these phosphorylations are Ca^{2+}-insensitive. Thus, a second objective of this study was to identify the protein kinase(s) that was(were) responsible for the calyculin A-induced phosphorylations. In a platelet lysate system, calyculin A caused an increase in the incorporation of [^{32}P]phosphate into p50. This phosphorylation event was identical to that observed in the intact platelet and was not mimicked by cAMP, cGMP, Ca^{2+}, or a Ca^{2+}/phospholipid/diacylglycerol mixture. Kinase activity was removed after the lysate was incubated with p13^{suc1}–Sepharose. This suggests that a p13^{suc1}-sensitive protein kinase, e.g., a cell cycle-dependent protein kinase, is responsible for the calyculin A-sensitive phosphorylation events. To support this notion, cdk2 was detected in p13^{suc1}–Sepharose precipitates using antibodies that were generated to conserve regions of the kinase.

Agonists and antagonists alter the phosphorylation state of platelet proteins (Lyons et al., 1975; Haslam et al., 1979). Consequently, the correlation between protein phosphorylations and regulation of platelet responses has been investigated vigorously by many laboratories [reviewed in Siess (1989)]. However, the extent to which protein phosphorylation regulates platelet responses still needs to be clarified. Studies have shown that the phosphorylation status of a limited number of proteins reflects the activation state of platelets (Kawamoto et al., 1989). Some of the enzymes that modulate the phosphorylation reactions have also been identified (Haslam et al., 1979; Rink et al., 1983; Kaibuchi et al., 1984). Two proteins having molecular weights of 20000 (p20) and 47000 (p47) have been shown to undergo agonist-induced phosphorylation and have been studied extensively in order to identify their functions as well as the role of specific protein kinases in controlling the activation process. From such studies, it is evident that protein kinase C is responsible for phosphorylating p47 (Nishizuka, 1984), whereas the Ca^{2+}/calmodulin-dependent enzyme MLCK[1] is responsible for phosphorylation of p20 (Dabrowska & Hartshorne, 1978). In contrast, activation of other protein

† This work was supported by Grants 90-085G and HL4489301 from the American Heart Association and NIH, respectively.

[1] Abbreviations: BAPTA, 1,2-bis(*o*-aminophenoxy)ethane-*N*,*N*,*N*′,*N*′-tetraacetic acid; EDTA, ethylenediaminetetraacetic acid; EGTA, ethylene glycol bis(β-aminoethyl ether)-*N*,*N*,*N*′,*N*′-tetraacetic acid; MLCK, myosin light chain kinase; Hepes, *N*-(2-hydroxyethyl)-piperazine-*N*′-2-ethanesulfonic acid; PGE_1, prostaglandin E_1; PGI_2 prostacyclin.

0006-2960/92/0431-6553$03.00/0